

ORIGINAL ARTICLE

Open Access



Cytotoxicity associated with acute and chronic administration of synthetic cannabinoids “Strox” in the brain, liver, heart, and testes of male albino rats: histological and immunohistochemical study

Wafaa M. Abdelmoneim¹, Marwa H. Bakr² , Nagwa M. Ghandour¹, Marwa Kh. Mohammed^{1*} , Mohamed Fawzy³, Abdelrahman G. Ramadan⁴ and Nora Z. Abdellah¹

Abstract

Background Synthetic cannabinoids are one of the largest groups of new psychoactive substances that invaded Egypt's drug abuse market over the past few years.

Aim Randomized controlled trial study to demonstrate the effects of acute and chronic toxicity by synthetic cannabinoid (Strox) on the brain, liver, heart, and testes in adult male albino rats through histopathological examination by light microscope and immunohistochemistry.

Methods Total number of fifty male albino rats were divided into five different groups, two control and three treated groups. Negative and positive control groups received distilled water and dimethyl sulfoxide, respectively, acute group received LD₅₀ (lethal dose 50) once and observed for 14 days, chronic group received 1/10 LD₅₀ for 3 months, and finally chronic withdrawal groups received 1/10 LD₅₀ for 3 months and then left 2 weeks without the substance to observe the withdrawal manifestations.

Results The current study revealed various histopathological changes in all organs with increased expression of cannabinoid receptor 1. The most important findings observed by light microscope examination were shrinkage and degenerative changes in Purkinje cells in brain sections, abnormalities in blood sinusoids and architecture in liver section, disruption in cardiac muscle fiber in heart sections, and finally testes showed irregularities in seminiferous tubules and germinal cells. Immunohistochemical staining for caspase-3 in the brain, liver, and heart showed weak-positive reaction in acute group and a strong reaction with chronic groups. Additionally, increase in collagen fiber was observed in sections of the liver and heart of chronic group.

Conclusions Synthetic cannabinoid sample (Strox) toxicity caused adverse effects on the brain, liver, heart, and testes as shown by increasing cannabinoid receptor 1 and caspase-3 expression.

Keywords Synthetic cannabinoids, New psychoactive substance, CB₁ receptor, Caspase-3, Withdrawal effect

*Correspondence:

Marwa Kh. Mohammed

marwakhalfa@aun.edu.eg; marwaa206@gmail.com

¹ Forensic Medicine and Clinical Toxicology Department, Faculty of Medicine, Assiut University, Assiut 71515, Egypt

² Histology and Cell Biology Department, Faculty of Medicine, Assiut University, Assiut 71515, Egypt

³ Neurology and Psychiatry Department, Faculty of Medicine, Assiut University, Assiut 71515, Egypt

⁴ Assiut University Hospital, Assiut 71515, Egypt



© The Author(s) 2023. **Open Access** This article is licensed under a Creative Commons Attribution 4.0 International License, which permits use, sharing, adaptation, distribution and reproduction in any medium or format, as long as you give appropriate credit to the original author(s) and the source, provide a link to the Creative Commons licence, and indicate if changes were made. The images or other third party material in this article are included in the article's Creative Commons licence, unless indicated otherwise in a credit line to the material. If material is not included in the article's Creative Commons licence and your intended use is not permitted by statutory regulation or exceeds the permitted use, you will need to obtain permission directly from the copyright holder. To view a copy of this licence, visit <http://creativecommons.org/licenses/by/4.0/>.

Background

New psychoactive substances (NPS) are unregulated designed drugs which generate effects similar to those of illegal drugs. They are developed to avoid the law (Rosado et al. 2018). Synthetic cannabinoids (SCs) are among the fastest growing and largest class of NPS, with hundreds of these chemicals increasingly emerging (Monti et al. 2022). These compounds are simply defined as molecules that bind to cannabinoid receptors (CB₁ and CB₂) and have the potential to modulate and regulate the activation of these receptors (Gregory et al. 2022). Despite SCs are often used as legal alternatives to natural cannabis which is under law control in Egypt, most SCs are more potent and full agonists of the cannabinoid receptors than the natural cannabis (European Monitoring Centre for Drugs and Drug Addiction [EMCDDA] 2009) (Weinstein et al. 2017).

Synthetic cannabinoids are not recently invented compounds. They were first invented in the 1970s not for abusive consumption but as novel therapeutic agents and research tools to explore the endocannabinoid system and testing their efficacy in curing pain and controlling appetite, blood pressure, and nausea (Di Marzo and Petrocellis 2006).

In the last few years, an herbal mixture containing SCs that invaded the drug abuse market in Egypt was named “Strox (El-Masry and Abdelkader 2021). Since legislation commenced to control one of these herbal mixtures after detection of SCs in them, many new analogs have been shown up on the market. Thus, new SCs containing herbal mixture are anticipated to be emerged in the markets to replace the banned ones, making the description of “dog chasing its tail” is the most suitable (Howlett et al. 2021).

The SCs are generally administered by smoking as a joint or in a water pipe (Alves et al. 2020). Smoking is preferred by the users because of the relatively quick onset of desirable effects and the allowance for titration to these effect (Auwärter et al., 2009). Currently, e-cigarette devices are used by young consumers and gaining a popularity (Castellanos and Gralnik 2016).

The United Nations Office on Drugs and Crime reported that 280 different substances have been identified worldwide as being SCs. Thus, SCs are considered the largest and the most heterogeneous class of NPS (Alves et al. 2020). Most SCs mixtures on the drug market have not been subjected to any in vivo testing, and only a limited amount of information is available in worldwide medical databases. Hence, their physiological and pharmacological effects are unknown (Alves et al. 2020; Assi et al. 2020). The aim of this work is to demonstrate the effects of acute and chronic toxicity by seized synthetic cannabinoids (Strox) on the brain, liver, heart, and testis in adult male albino rats through

histopathological examination by light microscope and immunohistochemistry.

Methods

Ethical approval

The experiments were conducted according to the protocol approved by the Medical Ethics Committee, Faculty of Medicine, Assiut University with the application of all directions with animal's dealing and according to the Guidelines of the National Institute of Health for Animal Care followed within the Faculty of Medicine, Assiut University, according to referenced authority (National Research Council (US) Committee for the Update of the Guide for the Care and Use of Laboratory Animals 2011).

Sample size calculation

This is sample size equation for the animal part by using open epi software ([://www.openepi.com/](http://www.openepi.com/)) and according to reference (Abass et al. 2017) with study power 80%, significance level 95%, size effect 60%, and confidence interval 95%: number for each group is 10 rats, and according to Ballantyne et al. (2009), the maximum accepted number of animals in group ranges from 6 to 10.

Chemicals and reagents

- *Synthetic cannabinoids*: In the form of Strox, sample was obtained by official request to the ministry of justice (seized samples). Sample was analyzed using gas chromatography/mass spectrophotometry (GC/MS). The compounds demonstrated were more than two-hundred compounds, presented are some of these ingredients: pyridine, 3-(1-methyl-2-pyrrolidinyl)-,(S)-(C₁₀H₁₄N₂); dihydromorphine; di(trimethylsilyl) ether; 3H-1,4-benzodiazepin 2-amino-7-chloro-5-phenyl-; 4-oxide, octadecanoic acid; 2-[(1-oxohexadecyl)oxy]ethyl ester; oleic acid; eicosyl ester; hexadecanoic acid; 2-(hexadecyloxy) ethyl ester; dasycarpidan-1-methanol; 6,8-dibromo-2-(3-pyridyl)-4-phenyl-quinazoline, and many indole containing compounds.
- *Tween 80*: (molecular weight 1310 g/mol, molecular formula C₆₄H₁₂₄O₂₆, CAS number 9005-65-6) and was purchased from Alpha Chemical Company, Egypt.
- *Dimethyl sulfoxide (DMSO)*: (molecular weight 78.14 g/mol, molecular formula (CH₃)₂SO or C₂H₆OS, CAS number: 67-68-5) and was purchased from Alpha Medical Group, Egypt. *Cannabinoid receptor-1 antibody (CB₁)* was purchased from (PA1-743, Thermo Scientific, USA).

- *Caspase-3 antibody* was purchased from Santa Cruz Biotechnology (Santa Cruz, CA, USA). *Inducible nitric oxide synthase (iNOS)* was purchased from (PA3-030A, Thermo Scientific, USA).
- *Biotinylated secondary antibody* was purchased from (Thermo Fisher Scientific Universal kit, Thermo Fisher Scientific Co., Fremont, CA, USA).
- *Calculation of the oral LD₅₀ of the synthetic cannabinoids (Strox)*

The LD₅₀ was calculated using the up-and-down procedure (UDP) for acute oral toxicity. As there was no available information to make a preliminary estimate of the LD₅₀ curve, computer simulations had suggested 175 mg/kg as a starting dose. This test consisted of a single-ordered dose progression in which rats were dosed once per time at least 48 h apart. The first animal which was tested received a dose step lesser than the amount of the LD₅₀ best estimate. Thereafter, the dose for the following animal is raised by (a factor of 3.2 times) the initial dose if the animal survives. On the other hand, if the animal dies, the next animal's dose is dropped by a similar dose progression. Before deciding how much to administer the next animal, each animal should be carefully examined for up to 48 h. To keep the number of animals low, a mix of stopping criteria was utilized, as well as altering the dosage pattern to limit the effect of a bad starting value or low slope. When one of these criteria was met, dosing was discontinued. Finally, approximation of the LD₅₀ and a confidence interval for the test were derived based on the state of all animals at termination (OECD, O 2000; OECD 2008).

Statistically estimated LD₅₀ based on long-term outcomes using the up-and-down procedure (UDP) for acute oral toxicity was 3194 mg/kg (approximate 95% confidence interval is 2000 to 5000, based on an assumed sigma of 0.5). A total number of 8 adult male albino rats weighing between 200 and 250 mg were used, which were chosen at random and kept in the animal house at Assiut University's Faculty of Medicine. The suggested doses by the software were 175, 550, 1750, 2000, and 5000 mg/kg. They received 1 ml of the synthetic cannabinoid's (Strox) extract dissolved in dimethyl sulfoxide (DMSO) (10% final volume), suspended in Tween 80 (20% final volume), and diluted in 0.9% NaCl (70% final volume) in a single dose by gavage (Renard et al. 2013). Short-term outcomes (first 48 h) and long-term outcomes (up to 14 days) were recorded. Calculation of the LD₅₀ is illustrated in Fig. 1.

Animals and experimental design

Fifty male albino rats were used; their weights were about 200–250 g. Moreover, rats were purchased from the animal breeding of Faculty of Medicine, Assiut University. Rats were housed in groups of five in clean, acceptable cages under conventional laboratory settings, which included an aerated room with an appropriate temperature (22 °C) and a 12-h light/dark cycle. Water and standard rodent diet (ground maize and bran) were freely available. Following 1 week of acclimatization, rats were randomly divided into 5 groups ($n = 10$) each:

- *Group 1* ($N = 10$) (negative control): Untreated rats received distilled water through gastric tube for about 90 days.

Calculation of the oral LD₅₀ of synthetic cannabinoids using up and down procedure

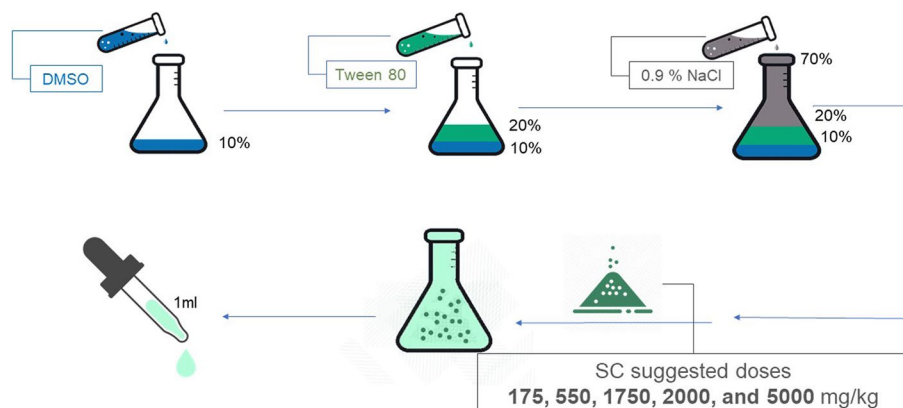


Fig. 1 Calculation of oral LD₅₀ of synthetic cannabinoids (Strox) using up-and-down-procedure (UDP)

- *Group 2* ($N = 10$) (positive control): Rats were given the same quantity of the solution used in dissolving Stox through a gastric tube 1 ml of dimethyl sulfoxide (DMSO) (10% final volume), suspended in Tween 80 (20% final volume), and diluted in 0.9% NaCl (70% final volume) for 90 days.
- *Group 3* ($N = 10$) (acute treated group): Rats received the calculated LD_{50} (equals 3194 mg/kg) once by gastric tube and were observed for 14 days for death or abnormal behavior.
- *Group 4* ($N = 10$) (chronic treated group): Rats were given a dose of synthetic cannabinoid (Strox) extract equal to 1/10 of the calculated LD_{50} by gastric tube dissolved in the abovementioned solution (Chopra et al. 2000). The dose was received once daily for about 90 days. Behavior and animal weight were observed. This time span corresponds to around 101 months or 8.5 years of human use (Huestis 2002).
- *Group 5* ($N = 10$) (chronic withdrawal group): Rats got a dose of synthetic cannabinoid (Strox) extract equal to 1/10 of the calculated LD_{50} by gastric tube dissolved in the abovementioned solution (Chopra et al. 2000). The dose was received once daily for about 90 days. Behavior and animal weight were observed. At the end of this period, rats will be left without the drug (abrupt withdrawal) for 14 days before sacrificing to observe the withdrawal symptoms.

All rats were decapitated by the end of the experiment, and specimens from the cerebellum, liver, heart (left ventricle), and testes were quickly removed and cut into small pieces, fixed in 10% formaldehyde solution, embedded in paraffin, and sliced at 5 μ m thickness and processed for histological and immunohistochemical examination.

Histopathological examination

Sections were stained with hematoxylin and eosin (H&E) to examine the morphological changes (Bancroft and Stevens 1990). The evaluation was done with a light microscope (Olympus, Bx50, Model Bx50F-3, SC09160, Tokyo, Japan). The observation criteria of histological feature are degenerative changing, including shrinkage or damage of Purkinje cells. At least five microscopic fields were evaluated at magnification $\times 400$ to score the specimens. Each specimen was scored using a scale (0: none, 1: mild, 2: moderate, and 3: severe). Picrosirius red (SR) stain was applied to demonstrate collagen fibers in the liver and heart (Dewald et al. 2003). The mean area % of collagen fibers in the liver and heart was determined using SR-stained sections. The measurements were performed using a $\times 10$ objective lens in five nonadjacent fields from five different sections per group.

Immunohistochemical examination

Paraffin sections were stained with *cannabinoid receptor 1 antibody* (CB_1) for the detection of endocannabinoids, *caspase-3* antibody for the detection of apoptotic cells, and *inducible nitric oxide synthase (iNOS)* antibody to detect iNOS. The sections were deparaffinized and rehydrated in descending concentrations of alcohol. Antigen was retrieved by heating in a citrate buffer for 10 min. Thereafter, all tissue sections were treated for 30 min in 3% H_2O_2 diluted in distilled water to abolish endogenous peroxidase activity. To decrease the nonspecific background, the sections were blocked with normal goat serum for 30 min. Then, they were incubated with the primary antibodies overnight at 4 °C. After washing in phosphate-buffered saline (PBS) buffer, the cells were incubated for 1 h at room temperature with a biotinylated secondary antibody. 3,3'-Diaminobenzidine (DAB) was used to visualize the process. The sections were dehydrated, cleaned, mounted on a coverslip, and examined under a light microscope after being counterstained with Meyer's hematoxylin. Negative control sections were set up by omitting the primary antibodies.

Immunohistochemical evaluation

Counting the number of cannabinoid receptor-1 (CB_1) immunopositive cells in the brain using the touch count method in immunostained sections at $\times 400$ magnification was performed. Scoring was done for both intensity and distribution (number of Purkinje cells) for each slide. The intensity of staining was graded from 0 to 3 as follows: no staining (0), weakly positive (1), moderately positive (2), and strongly positive (3). Then, the immunoreactivity score was calculated by multiplying the distribution and intensity. Thereafter, five randomly selected fields per microscopic slide were evaluated. The slides were photographed using a digital camera attached to a Leica universal microscope at the Histology Department, Faculty of Medicine, Assiut University. The images were analyzed on ImageJ version 1.52 k software.

Statistical analysis

SPSS version 19 was used for data entry and analysis. Analytic statistics in the form of ANOVA was used. P -values that are equal to or less than 0.05 were considered significant.

Results

Effects of acute and chronic toxicity, by synthetic cannabinoid (Strox), on animal weight and behavior changes

Activity level

The rats were hypoactive for 3 to 4 h after receiving the acute dose, as observed by their lack of interest in food

or their glancing from the cage to the stranger and total time mobile as measure of activity compared with the control group, but later became as active as control rats. However, chronic and withdrawal group rats did not show an observable change in activity in comparison with the control group.

Food intake

In comparison with the control group, the rats' food consumption increased slightly after chronic SC administration in the form of finishing food in the cage. Acute group's food intake decreased within the first 4 h after administration and then became like that of the control group until the end of the period of observation (14 days), while the withdrawal group did not show any significant change in food intake over the control group.

Weight

The weight of the animals of the chronic group observed in the study period was insignificantly increased compared to the control group, as shown in Fig. 2.

Histological and immunohistochemical results

We explored the effect of toxicity of synthetic cannabinoid sample (Strox) on the morphology of the brain, liver, heart, and testes.

Cerebellar cortex

Light microscopic examination of H&E Examination by light microscope of negative and positive control groups' sections stained with H&E stain showed a normal appearance of the cerebellum. Each cerebellar folium

is made up of three layers from outer to inner, respectively: molecular, Purkinje cell, and granular. The outer molecular layer appeared as a pale pink zone formed mainly of nerve fibers and a few scattered neuronal and glial cell bodies, while the middle Purkinje cell layer had large, pyriform Purkinje neuronal cells with large central oval nuclei. From the apical pole arises a dendritic tree extending into the molecular layer. Finally, the granular layer was formed of aggregation of small granule cells with rounded dark nuclei and scanty cytoplasm. These cells were separated by acidophilic areas called cerebellar glomeruli (Fig. 3 A, B).

In contrast, sections of the acute treated group revealed significant shrinkage of the Purkinje cell bodies with darkly stained nuclei and empty spaces surrounding them; others were distorted with ill-defined nuclei. In addition, some cells of molecular and granular layers appeared with deeply stained nuclei (Fig. 3C, Table 1). The chronic treated group showed degenerative changes in some Purkinje cells and shrinkages in others, leaving empty spaces surrounding them. Moreover, the granular layer revealed decreased packing of the nuclei; some nuclei appeared dense with irregular outlines (Fig. 3D). While the chronic withdrawal group revealed marked degenerative changes in Purkinje cells, some of them were lost, leaving empty spaces (Fig. 3E) in comparison with the control groups (Table 1).

Immunohistochemically stained sections for cannabinoid receptor 1 (CB1) Regarding immunohistochemically stained sections for cannabinoid receptor 1 (CB1), the negative and positive control groups showed strong positive immunoreactivity of Purkinje cells as well as

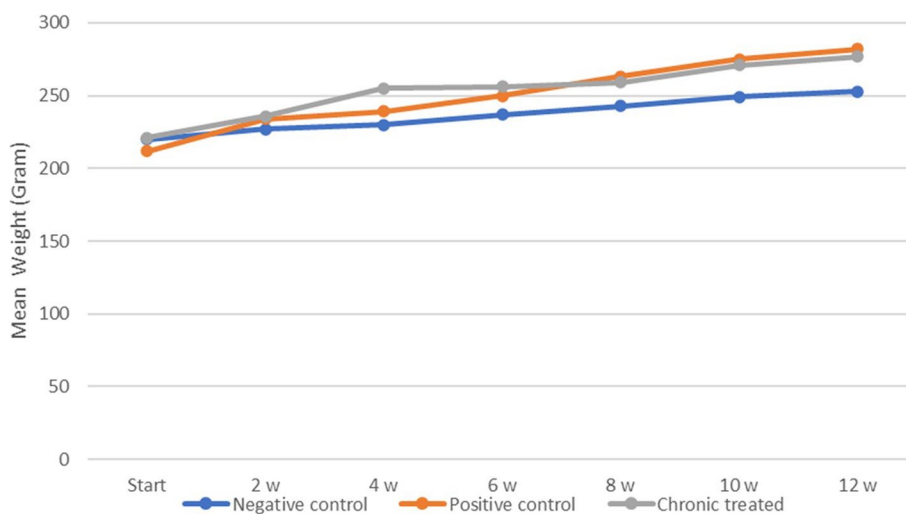


Fig. 2 Line chart demonstrates the difference in animal weight during periods of observation in the chronic study

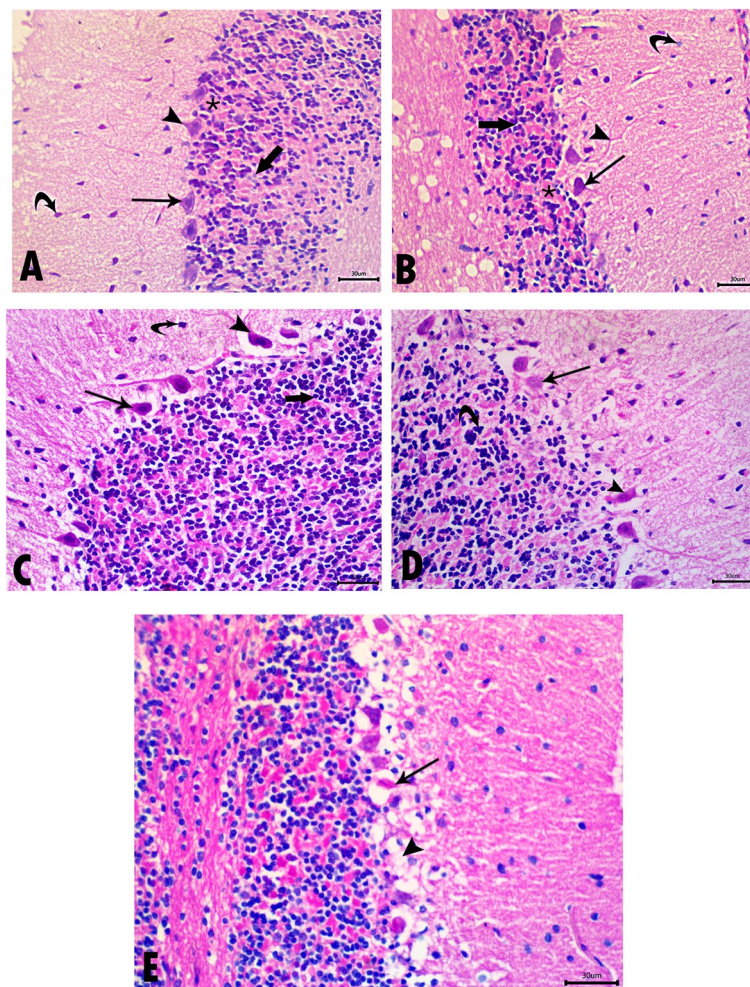


Fig. 3 Photomicrographs of sections in the cerebellar cortex stained with H&E ($\times 400$). **A** and **B** Negative and positive control groups show the three layers of the cerebellum. The outer molecular layer contains glial cells (curved arrows). The middle Purkinje cell layer has large, pyriform Purkinje neuronal cells with large central oval nuclei (arrows) and apparent cellular processes passing through the molecular layer (arrowheads). The inner granular layer shows an aggregation of small granule cells (thick arrows) separated by acidophilic areas (asterisk), representing the cerebellar glomeruli. **C** Acute treated group shows shrinkage of the Purkinje cell bodies with darkly stained nuclei and empty spaces surrounding them (arrowhead); others are distorted with small deeply stained nuclei (arrow). Some cells of molecular (curved arrow) and granular (thick arrow) layers appear with deeply stained nuclei. **D** Chronic treated group reveals marked degenerative changes in some Purkinje cells (arrow), and others are shrinkages leaving empty spaces surrounding them (arrowhead). Decreased packing of the nuclei in the granular layer is also detected. Some nuclei appear dense with irregular outlines (curved arrow). **E** Chronic withdrawal group shows degenerative changes in Purkinje cells (arrow), and some of them are lost, leaving empty spaces (arrowhead)

the nuclei of some cells in the molecular layer (Fig. 4 A, B). At the same time, the acute treated group showed a decrease in positive reactions in Purkinje cells (Fig. 4C). Moreover, the chronic treated group revealed few positive reactions in Purkinje cells (Fig. 4D). In comparison, the chronic withdrawal group showed a mild increase in positive reactions in Purkinje cells (Fig. 4E). Using ImageJ software to confirm the immunohistochemical data, the mean number of CB1 Purkinje-positive cells and immunohistochemical scoring was calculated. Highly significant reductions in the number and scoring of Purkinje

cells in acute, chronic, and chronic withdrawal groups were observed compared to negative and positive control groups ($P < 0.001$). Similarly, a highly significant difference with a reduction in the acute group compared to both chronic and chronic withdrawal groups with a P -value < 0.001 was also found. On the other hand, no significant difference was detected between the negative and positive control groups (Fig. 4E, Table 1).

Immunohistochemical staining for caspase-3 Immunohistochemical staining for caspase-3 showed negative

Table 1 Immunohistochemical and degenerative changes scoring difference between the studied groups

	Negative control Mean ± SD	Positive control Mean ± SD	Acute treated Mean ± SD	Chronic treated Mean ± SD	Chronic withdrawal Mean ± SD	p-value (between the groups)
Immunohistochemical score	25.67 ± 4.5	21.56 ± 2.9	7.56 ± 2.3	0.67 ± 1	1.89 ± 1.4	≤ 0.001
P-value 1		0.23	≤ 0.001	≤ 0.001	≤ 0.001	
P-value 2			≤ 0.001	≤ 0.001	≤ 0.001	
P-value 3				≤ 0.001	0.001	
P-value 4					0.878	
Degenerative changes scoring (damage or shrinkage of cells)	0 ± 0	0.38 ± 0.5	1.88 ± 0.6	2.88 ± 0.35	2.75 ± 0.46	≤ 0.001
P-value 1			≤ 0.001	≤ 0.001	≤ 0.001	
P-value 2			≤ 0.001	≤ 0.001	≤ 0.001	
P-value 3				0.001	0.004	
P-value 4					0.98	

P1, comparison between negative control and positive control, acute, chronic, chronic withdrawal groups; P2, comparison between positive control and acute, chronic, chronic withdrawal groups; P3, comparison between acute treated group and chronic and chronic withdrawal groups; P4, comparison between chronic treated group and withdrawal group. SD, standard deviation, P-value < 0.05 considered statistically significant. ANOVA test was used to compare the mean difference between groups

immunoreaction in cytoplasm and nuclei of cells in granular, molecular, and Purkinje cell layers of negative and positive control groups (Fig. 5 A, B). In contrast, the acute treated group showed few positive reactions in granular, molecular, and Purkinje cell layers (Fig. 5C). Additionally, the chronic treated group revealed strong positive reactions in cells of granular, molecular, and Purkinje cell layers (Fig. 5D). On the other hand, the chronic withdrawal group showed weak immunoreactivity in cells of granular and Purkinje cell layers compared to the chronic group (Fig. 5E).

Immunohistochemical staining for inducible nitric oxide synthase (iNOS) Immunohistochemical staining for inducible nitric oxide synthase (iNOS) demonstrated negative reactions in the cerebellar cortex of control animals (Fig. 6 A, B). However, iNOS-positive cells were observed mainly in the Purkinje cell layer as well as granular and molecular cell layers of treated animals (Fig. 6 C, D, and E).

Liver

Light microscopic examination of H&E Examination of H&E-stained sections of negative and positive control groups showed normal architecture of tightly packed cords of hepatocytes around the central vein. Hepatocytes looked polyhedral with acidophilic cytoplasm and rounded vesicular nuclei with prominent nucleoli, and others were binucleated. Blood sinusoids were found as a network between the plates of hepatocytes; they were lined by flattened endothelial cells (Fig. 7 A, B). While

the acute treated group revealed dilated congested blood sinusoids, most hepatocytes appeared with vacuolated cytoplasm (Fig. 7C). Additionally, the chronic treated group displayed obvious hepatic changes. The alternations were noted in the form of disturbed liver architecture with congested central veins and dilated congested blood sinusoids. In addition, hepatocytes appeared with vacuolated cytoplasm; some had degenerated nuclei, and others had irregularly shaped nuclei (Fig. 7D).

Moreover, the chronic withdrawal group revealed degenerated hepatocytes. Liver cells appeared with multiple large, coalesced vacuoles. Dilated central vein and dilated congested blood sinusoid were also seen (Fig. 7E).

Examination of picosirius red-stained (SR) sections Examination of picosirius red-stained sections showed few collagen fibers around the central vein and portal tract in the negative and positive control groups (Fig. 8 A, B). While in acute, chronic, and chronic withdrawal groups, there was an increase in collagen fibers deposition around central veins and portal tract compared to the control group (Fig. 8 C, D, E). The area % of collagen in the acute, chronic, and chronic withdrawal groups showed a highly significant increase in the area % of collagen compared with negative and positive control groups ($P < 0.001$); the SR staining showed more red-stained areas (Fig. 8F).

Immunohistochemically stained sections for cannabinoid receptor 1 (CB1) In immunohistochemically stained sections for cannabinoid receptor 1 (CB1), the negative and positive control groups showed few positive

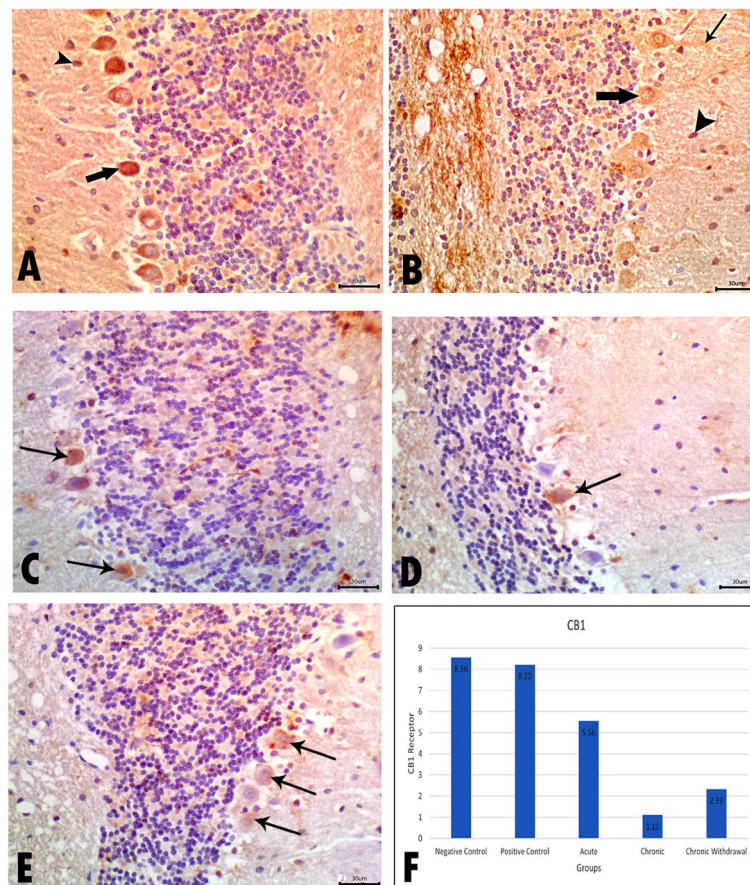


Fig 4 Photomicrographs of sections in the cerebellar cortex immunohistochemically stained with cannabinoid receptor 1 (CB1) ($\times 400$). **A** and **B** Negative and positive control groups show strong positive immunoreaction of Purkinje cells (thick arrow) as well as the nuclei of some cells in the molecular layer (arrowhead). The arrow points to the Purkinje dendrites in the molecular layer. **C** Acute treated group shows a decrease in positive reaction in Purkinje cells (arrows) compared to control groups. **D** Chronic treated group reveals few positive reactions in Purkinje cells (arrow). **E** Chronic withdrawal group shows a mild increase in positive reaction in Purkinje cells (arrows) compared to the chronic group. **F** The bar chart shows the quantitative estimation of the mean count of CB1-positive cells. Data are expressed as the means \pm SD; $P < 0.001$ for control groups vs acute, chronic, and chronic withdrawal groups

reactions in the cytoplasm of hepatocytes (Fig. 9 A, B). In comparison, the acute treated group showed an increase in the positive immune hepatocytes (Fig. 9C). Moreover, the chronic treated group revealed a marked increase in positive reaction in hepatocytes (Fig. 9D). On the other hand, the chronic withdrawal group showed decreased positive reactions in hepatocytes compared to the chronic group (Fig. 9E).

Immunohistochemical staining for caspase-3 In examination of caspase-3 immunostained liver sections, the negative and positive control groups showed negative expression in the cytoplasm of hepatocytes (Fig. 10 A, B). The acute treated group showed weak-positive immune expression in some hepatocytes (Fig. 10C). On the other hand, the chronic treated group revealed positive cells with higher caspase-3 expressions in most hepatocytes'

cytoplasm (Fig. 10D). On the contrary, the chronic withdrawal group showed the decreased caspase-3-positive expression in most hepatocytes (Fig. 10E).

Heart

Light microscopic examination of H&E Light microscopic examination of left ventricular wall sections of negative and positive control groups stained with H&E revealed normal cardiac morphology with branching and anastomosing cardiac muscle fibers. Moreover, cardiomyocytes had central vesicular nuclei and acidophilic sarcoplasm (Fig. 11 A, B). In contrast, the acute treated group showed disruption of some cardiac muscle fibers with congested blood vessels. Many deeply stained nuclei were also seen (Fig. 11C). Similarly, the chronic treated

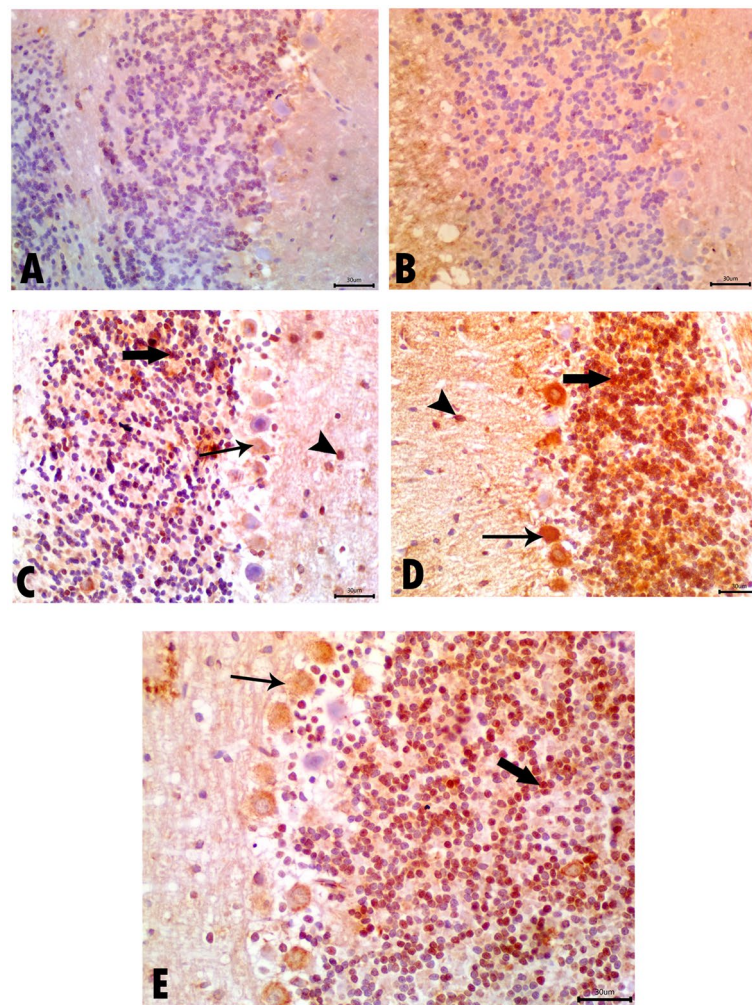


Fig. 5 Photomicrographs of sections in the cerebellar cortex immunohistochemically stained with caspase-3 ($\times 400$). **A** and **B** Negative and positive control groups show negative caspase-3 immunoreaction in cytoplasm and nuclei of cells in granular, molecular, and Purkinje cell layers. **C** Acute treated group shows few positive reactions in cells of granular (thick arrow), molecular (arrowhead), and Purkinje cell layers (arrow). **D** Chronic treated group reveals strong positive reaction in cells of granular (thick arrow), molecular (arrowhead), and Purkinje cell layers (arrow). **E** Chronic withdrawal group shows weak immunoreactivity in cells of granular (thick arrow) and Purkinje cell layers (arrow) compared to the chronic group

group showed dilated blood vessels in disorganized cardiac muscle fibers. Degeneration and discontinuity of cardiac muscle fibers with deeply stained irregular-shaped nuclei also appeared. Mononuclear cell infiltration was detected (Fig. 11D). Moreover, the chronic withdrawal group revealed dilated and congested blood vessels with disruption of cardiac muscle fibers and extravasation of blood cells (Fig. 11E).

Examination of picosirius red-stained (SR) sections In picosirius red-stained sections, the negative and positive control groups revealed few collagen fibers between cardiac muscle fibers (Fig. 12 A, B). However, in acute, chronic, and chronic withdrawal groups, there was an increase in

collagen fibers compared to control groups (Fig. 12 C, D, and E). The area % of the collagen in the acute, chronic, and chronic withdrawal groups showed a highly significant increase in the area % of collagen compared with negative and positive control groups ($P < 0.001$); the SR staining showed more red-stained areas (Fig. 12F).

Immunohistochemically stained sections for cannabinoid receptor 1 (CB1) In immunohistochemically stained sections for cannabinoid receptor 1 (CB1), the negative and positive control groups showed few positive reactions in the cytoplasm of cardiomyocytes (Fig. 13 A, B). Additionally, the acute treated group showed an increase in positive immune cardiomyocytes (Fig. 13C).

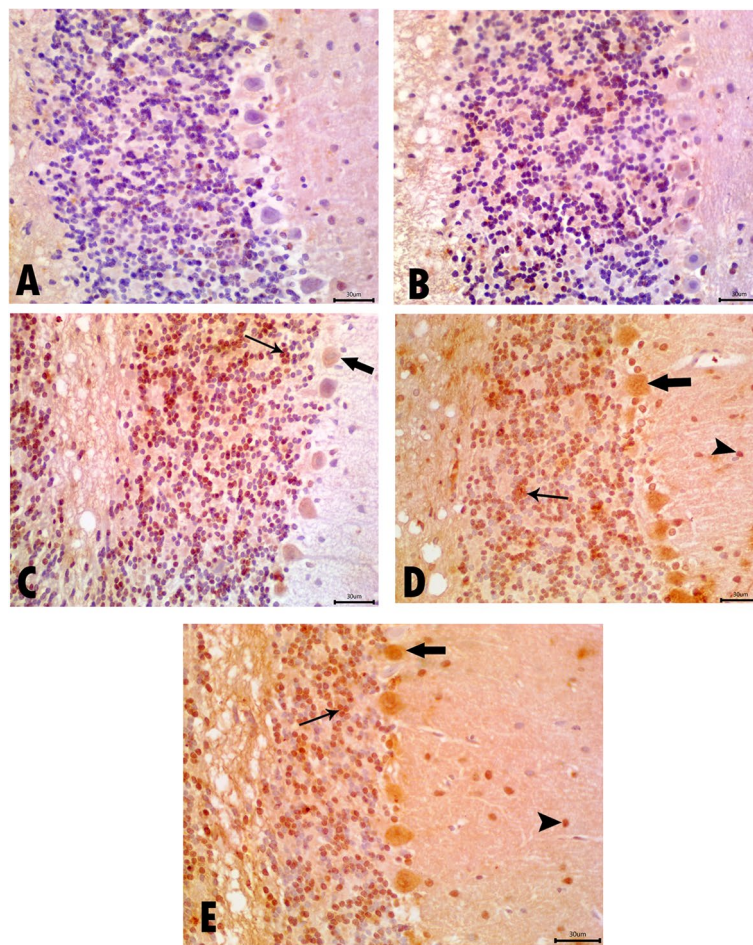


Fig. 6 Photomicrographs of sections in the cerebellar cortex immunohistochemically stained with inducible nitric oxide synthase (iNOS) ($\times 400$). **A** and **B** Negative and positive control groups show a negative reaction in the cerebellar cortex. **C** The acute treated group shows positive cells mainly in Purkinje cell (thick arrow) and granular cell layers (arrow). **D** and **E** Chronic treated and chronic withdrawal groups reveal strong positive reactions in cells of granular (arrow), molecular (arrowhead), and Purkinje cell layers (thick arrow)

Moreover, chronically treated and chronic withdrawal groups revealed a marked increase in positive reaction in cardiomyocytes (Fig. 13 D, E).

Immunohistochemical staining for caspase-3 Examination of caspase-3 immunostained left ventricular wall sections of the negative and positive control groups revealed negative expression in cardiomyocytes (Fig. 14 A, B). The acute treated group displayed weak-positive caspase-3 expression in cardiomyocytes (Fig. 14C). On the contrary, the chronic and chronic withdrawal groups revealed strong caspase-3 expression in cardiomyocytes (Fig. 14 D and E).

Testes

Light microscopic examination of H&E Light microscopic examination of H&E stained sections from the

testes of negative and positive control groups showed normal seminiferous tubules, which appeared regularly rounded or oval in shape and lined with stratified germinal epithelium formed of germinal cells and supporting Sertoli cells (Fig. 15 A, B). Primary spermatocytes were larger than spermatogonia and featured rounded black nuclei, while spermatogonia were small, spherical cells sitting on a basement membrane. Early-rounded and late-elongated spermatids were also observed. Sertoli cells had oval or triangle nuclei with a prominent nucleolus resting on the basement membrane and were observed in between the germ cells. Blood capillaries and clusters of interstitial Leydig cells were seen in the interstitial spaces between the seminiferous tubules (Fig. 15 A, B).

In contrast, the acute-treated group showed a reduction in the germinal epithelium with irregular

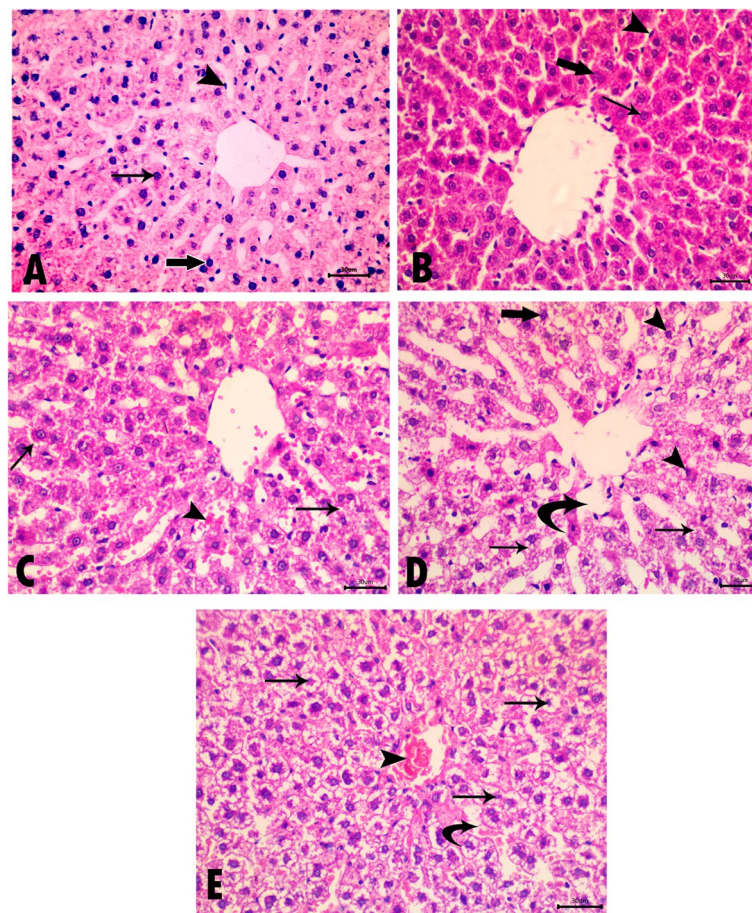


Fig. 7 Photomicrographs of sections in the liver stained with H&E ($\times 400$). **A** and **B** Negative and positive control groups show a normal architecture of tightly packed cords of hepatocytes around the central vein and blood sinusoid in between. Polyhedral hepatocytes with acidophilic cytoplasm and rounded vesicular nuclei with prominent nucleoli are seen (arrow). Some binucleated cells are also existing (thick arrow). Blood sinusoids are lined by flattened endothelial cells (arrowhead). **C** Acute treated group reveals dilated congested blood sinusoids (arrowhead), and most of the hepatocytes appear with vacuolated cytoplasm (arrows). **D** Chronic treated group showing disturbed liver architecture with dilated blood sinusoids (curved arrow). Hepatocytes appear with vacuolated cytoplasm (arrows); some have degenerated nuclei (arrowheads), and others have irregularly shaped nuclei (thick arrow). **E** Chronic withdrawal group reveals degenerated hepatocytes. Liver cells appear with multiple large, coalesced vacuoles and degenerated nuclei (arrows). Congested central vein (arrowhead) and dilated congested blood sinusoid (curved arrow) are also seen

seminiferous tubules and wide interstitial space (Fig. 15C). Additionally, the chronic-treated group revealed distortion of seminiferous tubules with vacuolation and disorganization of the seminiferous epithelium, exfoliation into the tubular lumen, and sloughing of germ cell nuclei. The tubular basement membrane was separated with interstitium deposition by an extremely acidophilic material (Fig. 15D). Chronic withdrawal group showed irregularity and distortion of seminiferous tubules. Some tubules revealed a decrease in the thickness of spermatogenic epithelium up to being depleted with few or no sperms. Vacuolar degeneration with dilated blood vessels in the interstitium was also noticed (Fig. 15E).

Discussion

New drugs with changing street names, containing synthetic cannabinoids, are gaining growing popularity among young adults in our country and worldwide. New cannabinoid mixtures are being continuously synthesized in the coming days to substitute the already illegal synthetic cannabinoids, resulting in a “dog chasing its tail” state (Fattore and Fratta 2011). Since little is known about in vivo effects of SCs currently available in market, this study describes both histopathological and immunohistochemical effects in male albino rats of the currently available SCs.

There was an acute onset of hypoactivity that was observed in the acute treated group which was also

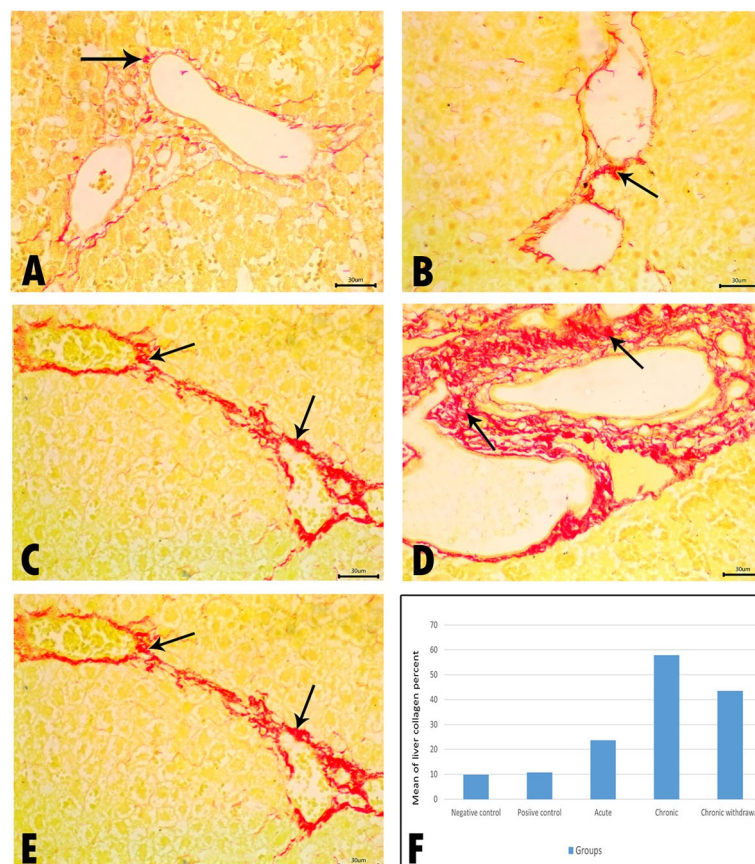


Fig. 8 Photomicrographs of sections in the liver stained with SR ($\times 400$). **A** and **B** Negative and positive control groups show few collagen fibers around portal tract (arrow). **C**, **D**, and **E**: Acute, chronic, and chronic withdrawal groups reveal increased in collagen fibers around portal tract (arrows) compared to the control groups. **F**: showing the mean area % of collagen fibers in all groups. Data are expressed as mean \pm SD; $P \leq 0.001$ for control groups vs acute, chronic, chronic withdrawal groups

observed after the effect of natural cannabis and other synthetic cannabinoids such as CP 55,940, AB-PIN-ACA, AB-FUBINACA, and JWH-018 (Arévalo et al. 2001; O'Shea et al. 2004; Quinn et al. 2008; Kevin et al. 2017). The observed increased weight gain in the chronic group in this study came in line with the significantly increased weight gain associated with sub-chronic cannabis use exhibited by Yassa et al. (2010)'s study but in controversy with other studies reported suppression of weight gain with chronic SCs consumption (Dalton et al. 2009; Klein et al. 2011).

Regarding cerebellar cortex examination between different groups, the acute treated group in the presenting study revealed shrinkage of the Purkinje cell bodies with darkly stained nuclei and empty spaces surrounding them; others were distorted with ill-defined nuclei. In addition, some cells of molecular and granular layers appeared with deeply stained nuclei. These results were in harmony with Abass et al. (2017), who reported the presence of shrunken vacuolated cells along with dense

cytoplasm and nuclei and irregular wide spaces around the cells with acute exposure to voodoo (synthetic cannabinoid), whereas the chronic treated group showed degenerative changes in some Purkinje cells and shrinkages of others leaving empty spaces surrounding them. Moreover, the granular layer revealed decreased packing of the nuclei; some nuclei appeared dense with irregular outlines. This agreed with the results of Mansour et al. (2020), who stated that with the sub-chronic exposure to voodoo extracts, all the cerebellum layers revealed the presence of vacuolated or shrunken neurons with darkly stained pyknotic or vesicular nuclei and vacuolated cytoplasm.

Cannabinoid CB_1 receptors are found all over the brain and mediate the central effects of cannabinoids (Lazenka et al. 2013). Concerning immunohistochemically stained sections for cannabinoid receptors 1 (CB_1), the negative and positive control groups showed strong positive immunoreaction of Purkinje cells in addition to the nuclei of some cells in the molecular layer. At

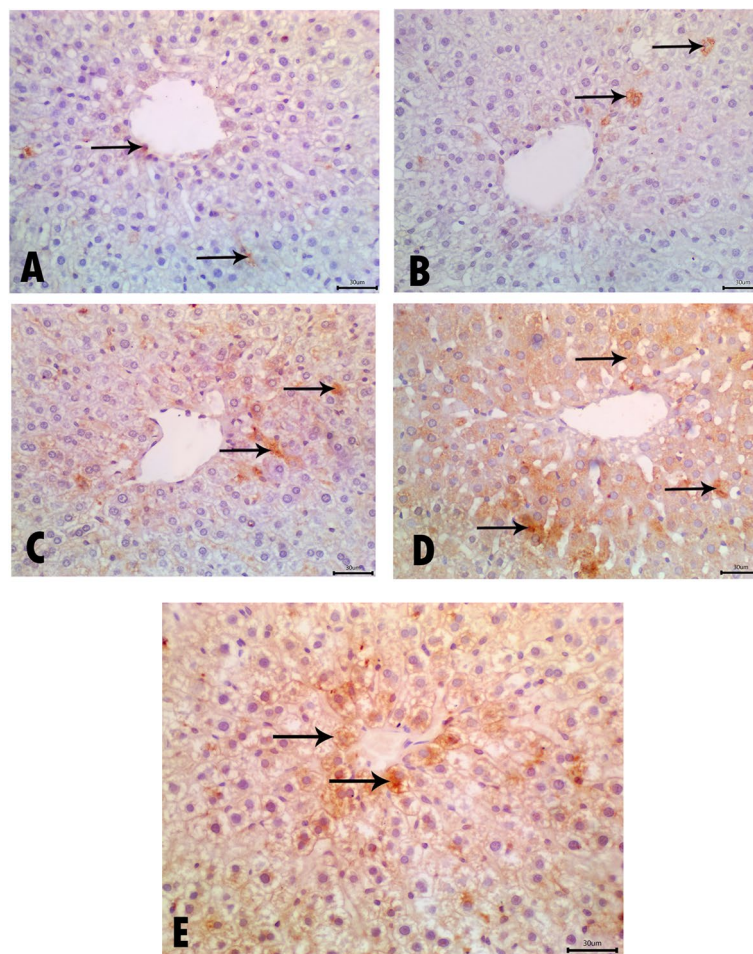


Fig. 9 Photomicrographs of sections in the liver immunohistochemically stained with cannabinoid receptor 1 (CB₁) (×400). **A** and **B** Negative and positive control groups show few positive reactions in the cytoplasm of hepatocytes (arrows). **C** The acute treated group shows positive immune hepatocytes (arrows). **D** Chronic treated group reveals an increased positive reaction in hepatocytes (arrows). **E** Chronic withdrawal group shows a decrease in positive reactions in hepatocytes (arrows) compared to the chronic group

the same time, the acute treated group demonstrated a positive reaction decrease in Purkinje cells. Moreover, the chronic treated group revealed few positive reactions in Purkinje cells. Morphometric analysis in this study revealed a highly significant reduction between the acute group and both chronic and chronic withdrawal groups. This can explain the tolerance associated with repeated use and the necessity of dosage increase to attain equal effects previously achieved by a lower dose. Breivogel et al. (2003) and Sim-Selley et al. (2006) reported a decrease in receptor expression in relation to chronic cannabinoid use. Also, Hirvonen et al. (2012) and Lazenka et al. (2013) found that frequent cannabis administration was associated with desensitization and downregulation of CB₁ receptors in some brain regions in humans and rats, respectively. However, Higuera-Matas et al. (2015) acknowledges the controversy of the long-term effects on the

endocannabinoid system resulting from chronic cannabinoid treatment.

In comparison, the chronic withdrawal group showed a mild increase of positive reactions in Purkinje cells. This was observed by Oliva et al. (2004) and Hirvonen et al. (2012), where time and regional responsiveness in cannabinoid CB₁ receptor gene expression confirmed the reversibility of the CB₁ expression after discontinuation of the substance. This was confirmed by Bosker et al. (2013) who found that after about 4 weeks of cannabis abstinence, the density of CB₁ receptors went back to normal in humans. This sustained reduction in the density of CB₁ receptor was associated with remarkable impairment of psychomotor functions, such as critical tracking and divided attention tasks for at least 3 weeks.

Histopathological results of the present study were supported by *immunohistochemical staining for caspase-3* as the acute treated group showed few positive

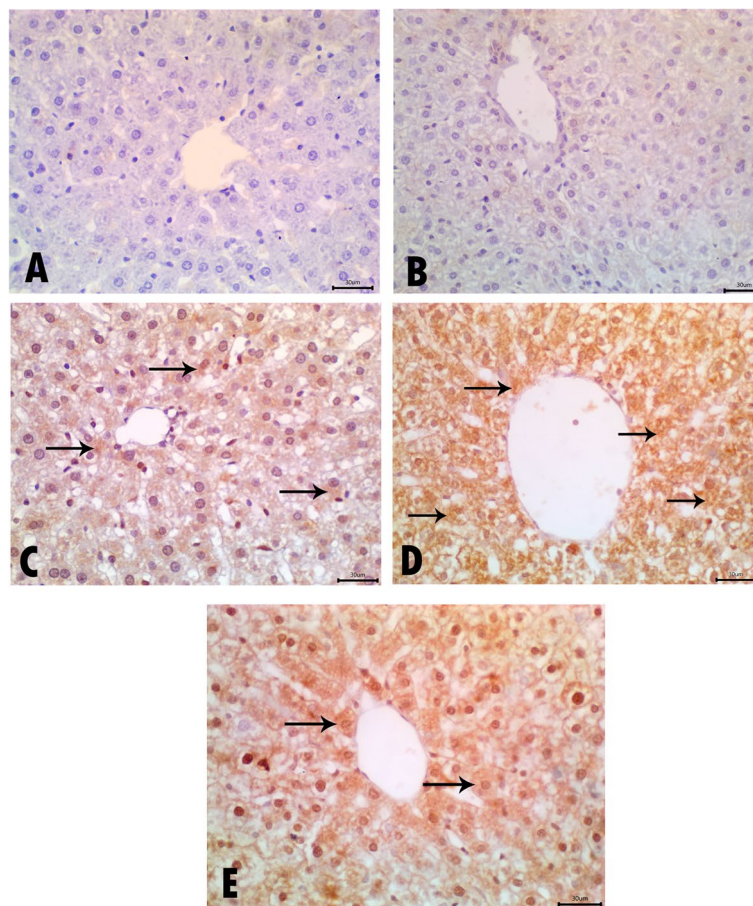


Fig. 10 Photomicrographs of sections in the liver immunohistochemically stained with caspase-3 ($\times 400$). **A** and **B** Negative and positive control groups show negative expression in the cytoplasm of hepatocytes. **C** The acute treated group shows positive immunoexpression in some hepatocytes (arrows). **D** Chronic treated group reveals positive cells with higher expression of caspase 3 in the cytoplasm of most of the hepatocytes (arrows). **E** Chronic withdrawal group shows the decreased caspase-3-positive expression in most hepatocytes (arrows)

reactions in granular, molecular, and Purkinje cell layers in comparison with negative immunoreaction in the negative and positive control groups. The CB_1 receptor mediates the synthetic cannabinoids' cytotoxicity towards the forebrain, and further caspase cascades may contribute significantly to the apoptosis caused by these synthetic cannabinoids after 2 h of exposure to different synthetic cannabinoids (Tomiya and Funada 2011; Tomiya and Funada 2014). Additionally, the chronic treated group revealed strong positive reactions in all layers. This neurotoxicity is associated with some cognitive deficits, for instance, impaired attention and memory loss associated with the chronic use of cannabinoids. Meanwhile, the chronic withdrawal group demonstrated weak immunoreactivity in granular and Purkinje cell layers compared to the chronic group.

Regarding immunohistochemical staining for inducible nitric oxide synthase (iNOS), nitric oxide (NO) is one of the inflammatory mediators released by

activated brain microglial cells. It plays a significant part in the central nervous system's antibacterial, antiviral, and antitumor activities (Cabral et al. 2001). iNOS-positive cells were mainly observed in the Purkinje cell layer in addition to granular and molecular cell layers of treated animals when compared to its absence in both control groups. This finding was in contrast with that observed by Cabral et al. (2001) and Fernández-López et al. (2006) where a cannabinoid agonist induced a potent neuroprotective effect in an *in vitro* model, who also reported that the neuroprotective effect increases if the substance is both CB_1 and CB_2 agonist than being only CB_1 or CB_2 agonist. That difference could be explained by the possible effect of the additive substance found with the used synthetic cannabinoids in this study (Strox).

Concerning liver findings difference among the studied groups, the acute treated group revealed dilated congested blood sinusoids, and most hepatocytes appeared

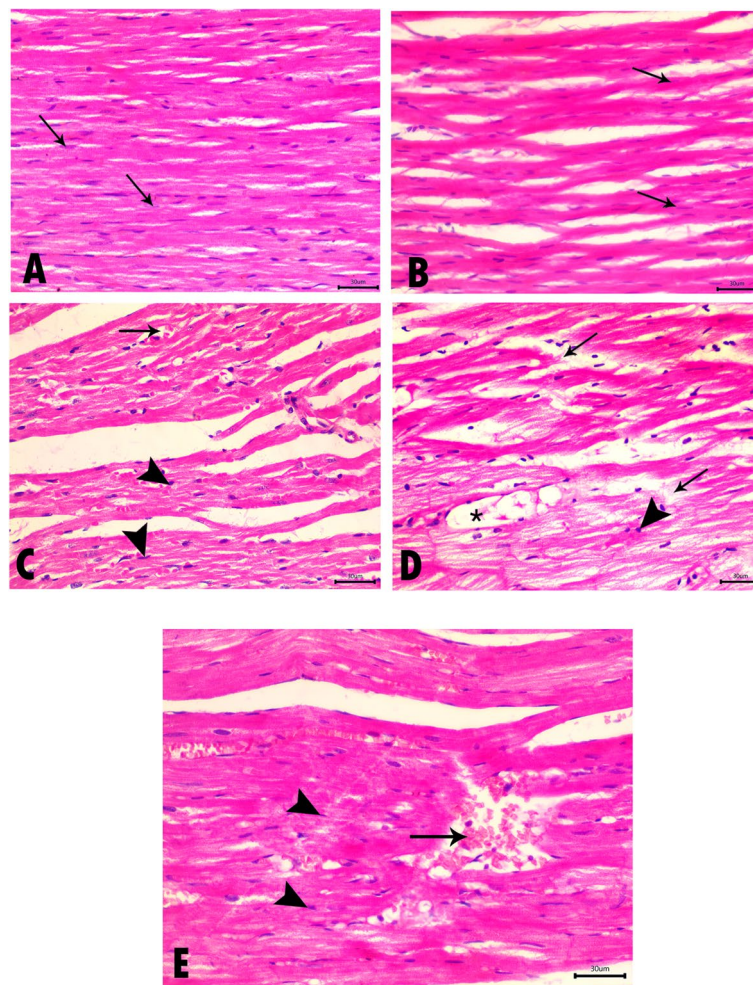


Fig. 11 Photomicrographs of the longitudinal sections of left ventricular heart muscles stained with H&E ($\times 400$). **A** and **B** Negative and positive control groups show normal heart morphology with branching and anastomosing cardiac muscle fibers. Cardiomyocytes have acidophilic sarcoplasm and central vesicular nuclei (arrows). **C** Acute treated group showing disruption of some cardiac muscle fibers with congested blood vessels (arrow). Many deeply stained nuclei are also seen (arrowheads). **D** Chronic treated group showing disorganized cardiac muscle fibers with dilated blood vessels (asterisk). Degeneration and discontinuity of cardiac muscle fibers (arrows) with deeply stained irregular-shaped nuclei also appear (arrowhead). Mononuclear cell infiltration is also detected. **E** Chronic withdrawal group reveals dilated and congested blood vessels with disruption of cardiac muscle fibers and extravasation of blood cells (arrow). Degeneration and irregularly shaped nuclei are also detected (arrowheads)

with vacuolated cytoplasm as compared to normal architecture of hepatocytes in both control groups, as well as Abass et al. (2017) results with voodoo in albino rats after acute exposure which showed severe congestion and macrovesicular steatosis with diffuse intracytoplasmic eosinophilic bodies. Recently, the results of another experimental study on albino rats for acute study showed the same finding of dilatation and congestion in blood sinusoids and hepatocytes hydropic degeneration, but their findings were dose dependent. Moreover, high doses showed disturbed liver architecture, and hepatic cell cords were widely separated due to dilatation of intrahepatic sinusoids (Mousa et al. 2021). Moreover, *picrosirius*

red stained in the present study showed more red-stained areas, increased collagen fibers deposition around central veins and portal tract, and an increase in the area % of collagen fibers in all acute, chronic, and chronic withdrawal groups as compared to few collagen deposition in both control groups. This came in contrast with the findings of Muñoz-Luque et al. (2008), who found that chronic stimulation of CB2 receptors by JWH-133 in rats having cirrhotic livers led to reduction of hepatic septal thickness and more preservation of hepatic parenchyma than non-treated cirrhotic animals and consequently a significant reduction in the fibrosis area percentage.

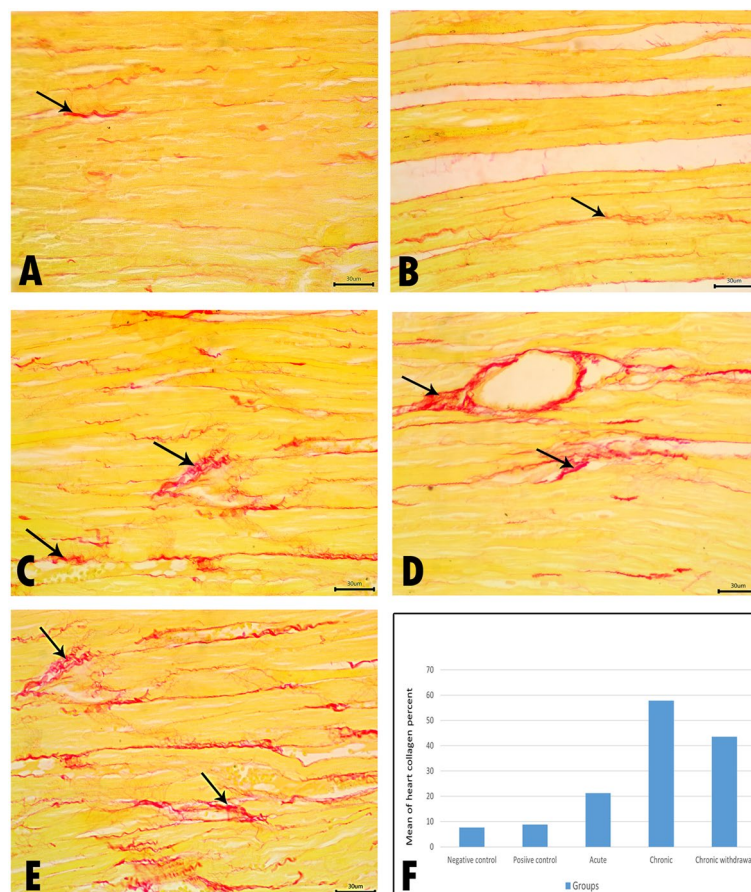


Fig. 12 Photomicrographs of the longitudinal sections of left ventricular heart muscles stained with SR ($\times 400$). **A** and **B** Negative and positive control groups show few collagen fibers between cardiac muscle fibers (arrow). While acute, chronic, and chronic withdrawal groups **C**, **D**, and **E**: reveal increased collagen fibers between cardiac muscle fibers compared to the control group (arrows). **F**: showing the mean area % of collagen fibers in all groups. Data are expressed as mean \pm SD; $P \leq 0.001$ for control groups vs acute, chronic and chronic withdrawal groups

Immunohistochemically stained liver sections for cannabinoid receptor 1 (CB₁) demonstrated that the negative and positive control groups showed few positive reactions in the cytoplasm of hepatocytes. That was also reported by Sánchez et al. (2003), who found that rat liver and spleen contain no or only low levels of CB₁ receptor normally. In comparison, both treated groups revealed an increase in positive immune cells. In contrast, the chronic withdrawal group demonstrated decreased positive reactions in hepatocytes compared to the chronic group. So, the use of synthetic cannabinoids was associated with activation of CB₁ receptors, which was reversible after discontinuation. CB₁ receptor activation in the liver was also found in many pathologies of the liver, which make CB₁ antagonists be investigated as a medication for many hepatic problems such as nonalcoholic liver cirrhosis (Wang et al. 2021). Furthermore, CB₁ receptor activation in the liver increased the incidence of fatty liver. This makes the use of SCs that are

CB₁ agonists for the long term associated with many hepatic pathologies (Pagotto et al. 2006).

Concerning immunohistochemical staining for caspase-3 of the liver, the chronic treated group revealed positive cells with higher caspase-3 expressions in most hepatocytes' cytoplasm as compared to the negative expression in control groups and weak expression in the acute treated group. On the contrary, the chronic withdrawal group showed decreased caspase-3-positive expression in most hepatocytes. This finding was similar to that of Muñoz-Luque et al. (2008), who found that treatment of cirrhotic rats with JWH-133 revealed significantly higher activated caspase-3 than in the vehicle group.

In this study, the left ventricular wall section findings of the acute treated group revealed disruption of some cardiac muscle fibers with congested blood vessels. In addition, many deeply stained nuclei were also seen. Similar changes were observed by Mousa et al. (2021) since they

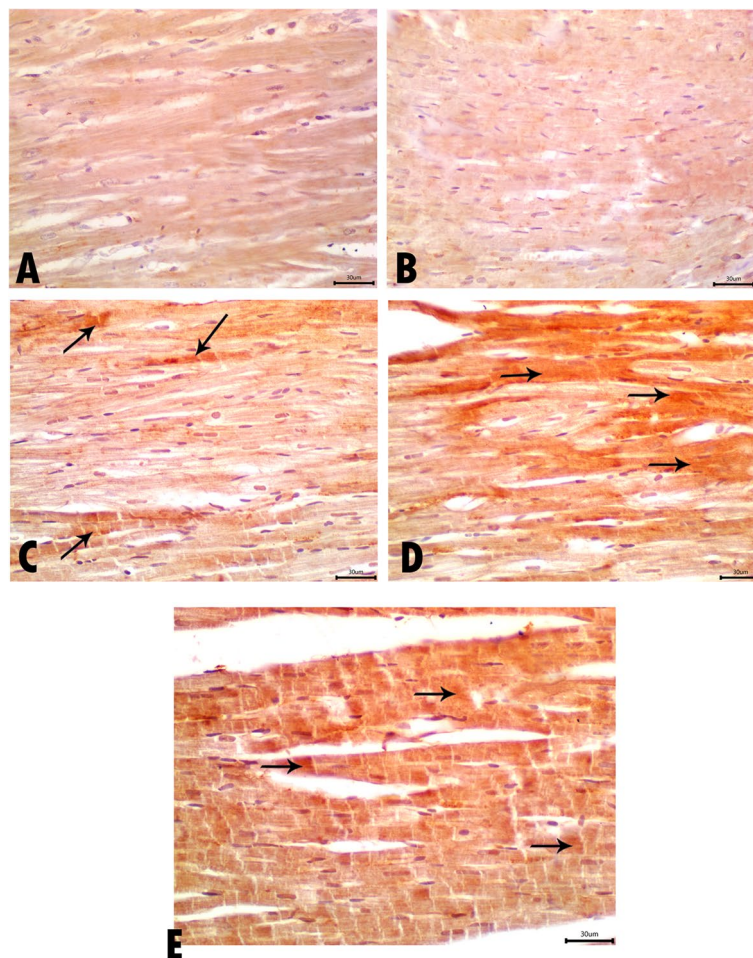


Fig. 13 Photomicrographs of sections in the heart immunohistochemically stained with cannabinoid receptor 1 (CB₁) (×400). **A** and **B** Negative and positive control groups show weak positive reactions in the cytoplasm of cardiomyocytes. **C** The acute treated group shows an increase in positive immune reaction in cardiomyocytes (arrows). **D** and **E** Chronic treated and chronic withdrawal groups reveal an increased positive reaction in cardiomyocytes (arrows)

observed dose-dependent changes in the form of pyknotic nuclei with acidophilic cytoplasm with an increase in the interstitial tissue thickness with areas of hemorrhage and cellular infiltration with loss of architecture and splitting into higher doses. Similarly, the chronic treated group showed disorganized and degenerated cardiac muscle fibers with dilated blood vessels. Additionally, picrosirius red-stained sections of the acute, chronic, and chronic withdrawal groups revealed an increase in the area % of collagen fibers compared to a few collagen depositions in both control groups. In line with our study, Slavic et al. (2013) have reported that CB₁ receptor antagonist decreases collagen accumulation and improves cardiac functions in the early and late stages after myocardial infarction.

Immunohistochemically stained sections for cannabinoid receptor 1 (CB₁) of the positive and negative control groups revealed few positive reactions in the cytoplasm

of cardiomyocytes. Additionally, acute, chronic, and chronic withdrawal groups revealed an increase in positive reactions in cardiomyocytes. *Moreover, examination of caspase-3 immunostained sections* of the acute treated group displayed weak-positive Caspase-3 expression in cardiomyocytes. On the contrary, the chronic and chronic withdrawal groups revealed strong caspase-3 expression in cardiomyocytes.

Findings of the present study were supported by animal studies from several researchers (Mukhopadhyay et al. 2010; Rajesh et al. 2010; Rajesh et al. 2012) who stated that CB₁ activation by endocannabinoids or synthetic agonists is related to cardiac inflammation, dysfunction, oxidative stress, and cell death associated with different forms of heart failure, shock, and atherosclerosis.

As regards testes results, morphological changes of the acute treated group revealed irregular seminiferous tubules with germinal epithelium reduction and

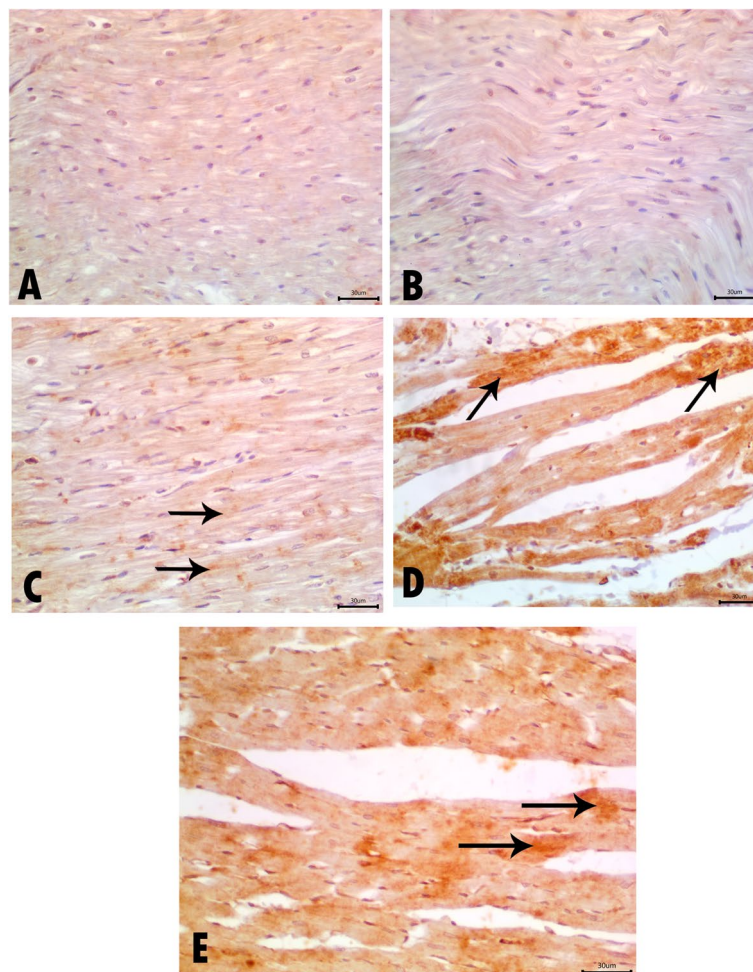


Fig. 14 Photomicrographs of sections in the heart immunohistochemically stained with caspase-3 ($\times 400$). **A** and **B** Negative and positive control groups show negative expression of caspase-3 in cardiomyocytes. **C** The acute treated group shows weak positive Caspase-3 expression in cardiomyocytes (arrows). **D** Chronic treated group reveals strong Caspase-3 expression in cardiomyocytes (arrows). **E** Chronic withdrawal group shows caspase-3-positive expression in cardiomyocytes (arrows)

wide interstitial space. This finding was harmonious with Mandal and Das (2010) and Mutluay et al. (2022). They found shrinkage of the seminiferous tubules and a reduced number of spermatogonia, which was statistically significant and dose related. Additionally, Mandal and Das (2010) observed significant basement membrane damage with the complete arrest of spermatogenesis. Moreover, the chronic treated group revealed distortion of seminiferous tubules with vacuolation and disorganization of the seminiferous epithelium, sloughing germ cells nuclei, and exfoliation into the tubular lumen. Furthermore, highly acidophilic material deposition in the interstitium and tubular basement membrane separation was also detected. This was in line

with the findings of Yassa et al. (2010) in sub-chronic toxicity of natural cannabis, where they observed irregularity and disruption of the basement membrane. Moreover, some seminiferous tubules revealed giant cells in its lumen, and the spermatogenic cells demonstrated small-dense nuclei with vacuolated and degenerated cytoplasm.

Additionally, Pagotto et al. (2006) discussed the hypothalamus-pituitary-gonadal axis regulation done by the endocannabinoid system both in males and in females, which can explain the effect of cannabinoid drugs on fertility. However, human studies had not correlated cannabinoid use and this negative impact (Fonseca and Rebelo 2021). And the concurrent consumption of other illicit drugs,

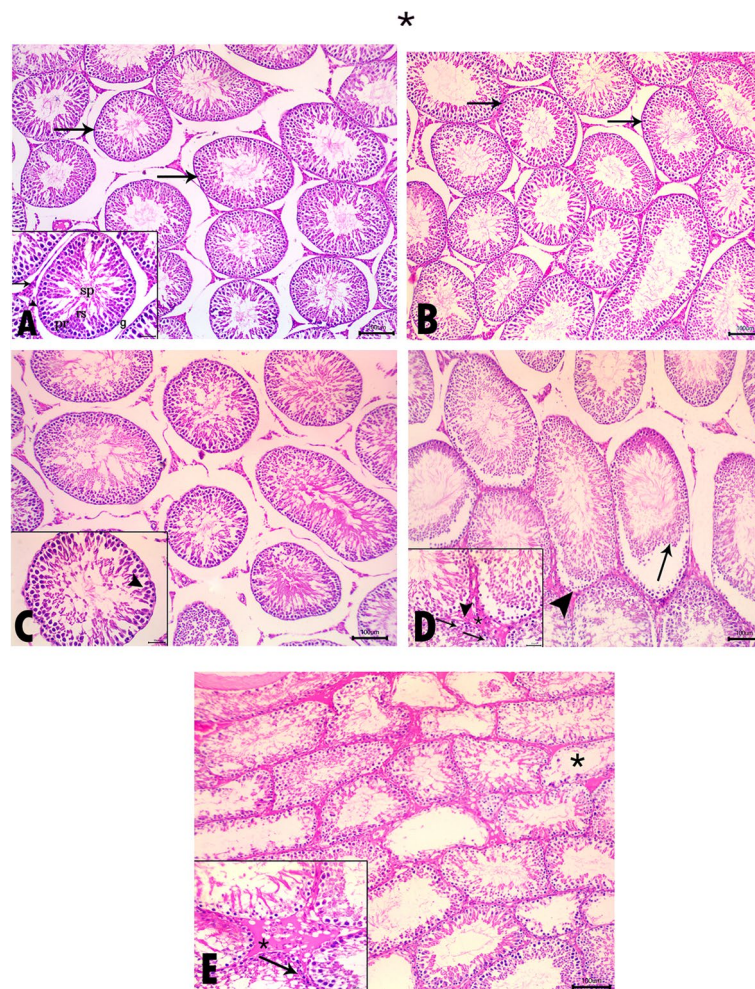


Fig. 15 Photomicrographs of sections in the testes stained with H&E ($\times 100$, inset $\times 400$). **A** and **B** Negative and positive control groups show normal seminiferous tubules (arrows) lined with stratified epithelium and separated by loose interstitial connective tissue. **Inset**; primary spermatocytes (pr), spermatogonia (g), round spermatids (rs), and sperms (sp). Sertoli cells (arrowhead) and Leydig cells (arrow). **C** Acute treated group showing seminiferous tubules with wide interstitial space. **Inset**; show reduction in the germinal epithelium (arrowhead). **D** Chronic treated group reveals distortion of seminiferous tubules, sloughing of germ cells nuclei, and exfoliation into the tubular lumen (arrow). Tubular basement membrane separation (arrowhead) is also seen. **Inset**; show vacuolation (arrows) with disorganized seminiferous epithelium. Congested blood vessels (arrowhead) and interstitium deposition by an extremely acidophilic material (asterisk). **E** Chronic withdrawal group shows irregularity and distortion of seminiferous tubules. Some tubules show a decrease in the thickness of spermatogenic epithelium up to depletion with few or no sperms (asterisk). **Inset**; revealed vacuolar degeneration (arrow) with dilated blood vessels and interstitium deposition by extremely acidophilic material (asterisk)

alcohols, and cigarettes smoking which also may harm fertility makes it difficult to confirm the correlation (Singh et al. 2020).

The chronic withdrawal group showed irregularity and distortion of seminiferous tubules. Additionally, some tubules revealed a spermatogenic epithelium thickness reduction up to depletion with no or few sperms. On the contrary, Mandal and Das (2010) reported a full recovery of testicular cell function and spermatogenesis in mice after 45 days of cannabis drug treatment (which is longer than the 14-day duration of the current study).

Conclusions

SCs with its numerous street names are gaining a growing popularity in Egypt with unpredictable sequels. Strox “as known in Egyptian street” is one of these SCs containing mixtures that were commonly abused and seized between addicts in recent years. Significant changes were found in the brain, liver, heart, and testes of male albino rats exposed to acute and chronic SCs (Strox). Notably, observed damage was less severe in the acute group compared to the chronic group. On the other hand, only a slight less severity was found in the withdrawal group compared to the chronically treated group. Additionally, downregulation

of CB₁ receptors in the brain determines the development of tolerance associated with chronic use of SCs. It also was demonstrated that the downregulation of these receptors was reversible as evidenced in the withdrawal group. Conclusively, the present study clearly shows that overactivation of the endocannabinoid system using strox affects the brain, heart, liver, and testes that may lead to severe complications and death.

Abbreviations

CB ₁	Cannabinoid receptor 1
CB ₂	Cannabinoid receptor 2
CP	Charles Pfizer
DAB	Diaminobenzidine
DMSO	Dimethyl sulfoxide
GC/MS	Gas chromatography/mass spectrophotometry
H&E	Hematoxylin and eosin
iNOS	Inducible nitric oxide synthase
JWH	John W. Huffman
LD ₅₀	Lethal dose 50
NO	Nitric oxide
NPS	New psychoactive substances
OECD	Organisation for Economic Co-operation and Development
PBS	Phosphate-buffered saline
SCs	Synthetic cannabinoids
SR	Picrosirius red
UDP	Up-and-down procedure

Acknowledgements

Not applicable.

Authors' contributions

WMA and NMG were the supervisor. MHB, AGR, NZA, and MKM contributed in writing the manuscript. MKM and NZA calculated the LD₅₀. MHB performed the histological examination. MHB, MF, and MKM prepared figures. The authors read and approved the final manuscript.

Funding

The authors declare that no funds, grants, or other support were received during the preparation of this manuscript.

Availability of data and materials

The datasets used and/or analyzed during the current study are available from the corresponding author on reasonable request.

Declarations

Ethics approval and consent to participate

The experiments were conducted according to the protocol approved by the Medical Ethics Committee, Faculty of Medicine — Assiut University.

Consent for publication

Not applicable.

Competing interests

The authors declare that they have no competing interests.

Received: 19 August 2022 Accepted: 29 January 2023

Published online: 09 February 2023

References

- Abass M, Hassan M, Abd Elhaleem M, Abd Elaziz H, Abd-Allah R (2017) Acute toxicity of a novel class of hallucinogen. *Ain Shams J Forensic Med Clin Toxicol* 28(1):62–73. <https://doi.org/10.21608/ajfm.2017.18280>
- Alves VL, Gonçalves JL, Aguiar J, Teixeira HM, Câmara JS (2020) The synthetic cannabinoids phenomenon: from structure to toxicological properties. A review. *Crit Rev Toxicol* 50(5):359–382. <https://doi.org/10.1080/10408444.2020.1762539>
- Arévalo C, de Miguel R, Hernández-Tristán R (2001) Cannabinoid effects on anxiety-related behaviours and hypothalamic neurotransmitters. *Pharmacol Biochem Behav* 70(1):123–131. [https://doi.org/10.1016/s0091-3057\(01\)00578-0](https://doi.org/10.1016/s0091-3057(01)00578-0)
- Assi S, Marshall D, Bersani FS, Corazza O (2020) Uses, effects and toxicity of synthetic cannabinoids from the perspective of people with lived experiences. *J Psychoactive Drugs* 52(3):237–247. <https://doi.org/10.1080/02791072.2020.1723748>
- Auwärter V, Dresen S, Weinmann W, Müller M, Pütz M, Ferreirós N (2009) 'Spice' and other herbal blends: harmless incense or cannabinoid designer drugs? *J Mass Spectrom* 44(5):832–837. <https://doi.org/10.1002/jms.1558>
- Ballantyne B, Marrs TC, Syversen T (2009) *General and applied toxicology*. 3rd ed., 6 Vols. Wiley-Blackwell, Oxford
- Bancroft JD, Stevens A (1990) *Theory and practice of histological techniques*, 17 vols. Churchill Livingstone, Edinburgh
- Bosker WM, Karschner EL, Lee D, Goodwin RS, Hirvonen J, Innis RB et al (2013) Psychomotor function in chronic daily cannabis smokers during sustained abstinence. *PLoS One* 8(1):e53127:1–7. <https://doi.org/10.1371/journal.pone.0053127>
- Breivogel CS, Scates SM, Beletskaya IO, Lowery OB, Aceto MD, Martin BR (2003) The effects of delta9-tetrahydrocannabinol physical dependence on brain cannabinoid receptors. *Eur J Pharmacol* 459(2–3):139–150. [https://doi.org/10.1016/s0014-2999\(02\)02854-6](https://doi.org/10.1016/s0014-2999(02)02854-6)
- Cabral GA, Harmon KN, Carlisle SJ (2001) Cannabinoid-mediated inhibition of inducible nitric oxide production by rat microglial cells: evidence for CB1 receptor participation. *Adv Exp Med Biol* 493:207–214. https://doi.org/10.1007/0-306-47611-8_24
- Castellanos D, Gralnik L (2016) Synthetic cannabinoids 2015: an update for pediatricians in clinical practice. *World J Clin Pediatr* 5(1):16–24
- Chopra S, Soni R, Chopra A (2000) A computer program for determination of LD₅₀ using dBase/Foxpro. *Indian J Pharm* 32(6):390
- Dalton VS, Wang H, Zavitsanou K (2009) HU210-induced downregulation in cannabinoid CB1 receptor binding strongly correlates with body weight loss in the adult rat. *Neurochem Res* 34(7):1343–1353. <https://doi.org/10.1007/s11064-009-9914-y>
- Dewald O, Frangogiannis NG, Zoerlein M, Duerr GD, Klemm C, Knuefermann P et al (2003) Development of murine ischemic cardiomyopathy is associated with a transient inflammatory reaction and depends on reactive oxygen species. *Proc Natl Acad Sci U S A* 100(5):2700–2705. <https://doi.org/10.1073/pnas.0438035100>
- Di Marzo V, Petrocellis L (2006) Plant, synthetic, and endogenous cannabinoids in medicine. *Annu Rev Med* 57:553–574
- El-Masry M, Abdelkader S (2021) Clinical profile of designer drug "Strox" intoxicated cases presented to poison control center Ain Shams University, Egypt from first of January 2017 to end of January 2018. *Ain Shams J Forensic Med Clin Toxicol* 36(1):98–105. <https://doi.org/10.21608/ajfm.2021.138857>
- European Monitoring Centre for Drugs and Drug Addiction [EMCDDA] (2009). "Understanding the "Spice" phenomenon". Thematic paper ed: Office for Official Publications of the European Communities. <https://www.emcdda.europa.eu>. Accessed 20 Sep 2020. 1–25
- European Monitoring Centre for Drugs and Drug Addiction (2021) European drug report: trends and developments https://www.emcdda.europa.eu/publications/edr/trends-developments/2021_en. Accessed 13 Sep 2021
- Fattore L, Fratta W (2011) Beyond THC: the new generation of cannabinoid designer drugs. *Front Behav Neurosci* 5:60. <https://doi.org/10.3389/fnbeh.2011.00060>
- Fernández-López D, Martínez-Orgado J, Nuñez E, Romero J, Lorenzo P, Moro MA, Lizasoain I (2006) Characterization of the neuroprotective effect of the cannabinoid agonist WIN-55212 in an in vitro model of hypoxic-ischemic brain damage in newborn rats. *Pediatr Res* 60(2):169–173. <https://doi.org/10.1203/01.pdr.0000228839.00122.6c>
- Fonseca BM, Rebelo I (2021) Cannabis and cannabinoids in reproduction and fertility: where we stand. *Reprod Sci*. <https://doi.org/10.1007/s43032-021-00588-1>
- Gregory TT, O'Malley K, Medina-Kirchner C, Guàrdia MG, Hart CL (2022) In: Akerele E (ed) *Cannabinoids: the case for legal regulation that permits*

- recreational adult use. Substance and non-substance related addictions: a global approach. Springer International Publishing, Cham, pp 149–160. https://doi.org/10.1007/978-3-030-84834-7_13
- Higuera-Matas A, Ucha M, Ambrosio E (2015) Long-term consequences of perinatal and adolescent cannabinoid exposure on neural and psychological processes. *Neurosci Biobehav Rev* 55:119–146. <https://doi.org/10.1016/j.neubiorev.2015.04.020>
- Hirvonen J, Goodwin RS, Li CT, Terry GE, Zoghbi SS, Morse C et al (2012) Reversible and regionally selective downregulation of brain cannabinoid CB1 receptors in chronic daily cannabis smokers. *Mol Psychiatry* 17(6):642–649. <https://doi.org/10.1038/mp.2011.82>
- Howlett A, Thomas B, Huffman J (2021) The spicy story of cannabimimetic indoles. *Molecules*. 26(20):6190:1-30
- Huestis MA (2002) Cannabis(marijuana)- effects on human behavior and performance. *Forensic Sci Rev* 14(1):15–60 PMID: 26256486
- Kevin RC, Wood KE, Stuart J, Mitchell AJ, Moir M, Banister SD et al (2017) Acute and residual effects in adolescent rats resulting from exposure to the novel synthetic cannabinoids AB-PINACA and AB-FUBINACA. *J Psychopharmacol* 31(6):757–769. <https://doi.org/10.1177/0269881116684336>
- Klein C, Karanges E, Spiro A, Wong A, Spencer J, Huynh T, et., al. (2011) Cannabidiol potentiates Δ^9 -tetrahydrocannabinol (THC) behavioural effects and alters THC pharmacokinetics during acute and chronic treatment in adolescent rats. *Psychopharmacology* 218(2):443–457. <https://doi.org/10.1007/s00213-011-2342-0>
- Lazenka MF, Selley DE, Sim-Selley LJ (2013) Brain regional differences in CB1 receptor adaptation and regulation of transcription. *Life Sci* 92(8-9):446–452. <https://doi.org/10.1016/j.lfs.2012.08.023>
- Mandal TK, Das NS (2010) Testicular toxicity in cannabis extract treated mice: association with oxidative stress and role of antioxidant enzyme systems. *Toxicol Ind Health* 26(1):11–23. <https://doi.org/10.1177/0748233709354553>
- Mansour GN, Hassan MZ, Nafea OE, Mohamed MZ (2020) The sub chronic toxic effect of voodoo extract on the central nervous system in adult male albino rats. *EJFSAT*. 20(2):1–13. <https://doi.org/10.21608/EJFSAT.2020.14782.1085>
- Monti MC, Zeuglin J, Koch K, Milenkovic N, Scheurer E, Mercer-Chalmers-Bender K (2022) Adulteration of low-delta-9-tetrahydrocannabinol products with synthetic cannabinoids: results from drug checking services. *Drug Test Anal* 14(6):1026–1039. <https://doi.org/10.1002/dta.3220>
- Mousa R, Gebri S, Masoud K, Radwan R, Mohamad S (2021) Acute toxic effects of AB-CHMINACA on lung, heart and liver: an experimental pilot study. *Ain Shams J Forensic Med Clin Toxicol* 37(2):128–135. <https://doi.org/10.21608/AJFM.2021.182715>
- Mukhopadhyay P, Rajesh M, Bátkai S, Patel V, Kashiwaya Y, Liaudet L et al (2010) CB1 cannabinoid receptors promote oxidative stress and cell death in murine models of doxorubicin-induced cardiomyopathy and in human cardiomyocytes. *Cardiovasc Res* 85(4):773–784. <https://doi.org/10.1093/cvr/cvp369>
- Muñoz-Luque J, Ros J, Fernández-Varo G, Tugues S, Morales-Ruiz M, Alvarez CE et al (2008) Regression of fibrosis after chronic stimulation of cannabinoid CB2 receptor in cirrhotic rats. *J Pharmacol Exp Ther* 324(2):475–483. <https://doi.org/10.1124/jpet.107.131896>
- Mutluay D, Güngör S, Tenekeci G, Köksöy S, Çoban C (2022) Effects of synthetic (JWH-018) cannabinoids treatment on spermatogenesis and sperm function. *Drug Chem Toxicol* 45(1):215–222. <https://doi.org/10.1080/01480545.2019.1680686>
- National Research Council (US) Committee for the Update of the Guide for the Care and Use of Laboratory Animals (2011) Guide for the care and use of laboratory animals, 8th edn. National Academies Press (US), Washington (DC)
- OECD (2008) OECD factbook 2008: economic, environmental and social statistics, publications de l'OCDE
- OECD, O (2000) Guidance document on acute oral toxicity testing. OECD, Paris
- Oliva JM, Ortiz S, Palomo T, Manzanares J (2004) Spontaneous cannabinoid withdrawal produces a differential time-related responsiveness in cannabinoid CB1 receptor gene expression in the mouse brain. *J Psychopharmacol* 18(1):59–65. <https://doi.org/10.1177/0269881104040238>
- O'Shea M, Singh ME, McGregor IS, Mallet PE (2004) Chronic cannabinoid exposure produces lasting memory impairment and increased anxiety in adolescent but not adult rats. *J Psychopharmacol* 18(4):502–508. <https://doi.org/10.1177/026988110401800407>
- Pagotto U, Marsicano G, Cota D, Lutz B, Pasquali R (2006) The emerging role of the endocannabinoid system in endocrine regulation and energy balance. *Endocr Rev* 27(1):73–100. <https://doi.org/10.1210/er.2005-0009>
- Quinn HR, Matsumoto I, Callaghan PD, Long LE, Arnold JC, Gunasekaran N, et., al. (2008) Adolescent rats find repeated delta(9)-THC less aversive than adult rats but display greater residual cognitive deficits and changes in hippocampal protein expression following exposure. *Neuropsychopharmacology*. 33(5):1113–1126. <https://doi.org/10.1038/sj.npp.1301475>
- Rajesh M, Mukhopadhyay P, Haskó G, Liaudet L, Mackie K, Pacher P (2010) Cannabinoid-1 receptor activation induces reactive oxygen species-dependent and -independent mitogen-activated protein kinase activation and cell death in human coronary artery endothelial cells. *Br J Pharmacol* 160(3):688–700. <https://doi.org/10.1111/j.1476-5381.2010.00712.x>
- Rajesh M, Bátkai S, Kechrid M, Mukhopadhyay P, Lee WS, Horváth B et al (2012) Cannabinoid 1 receptor promotes cardiac dysfunction, oxidative stress, inflammation, and fibrosis in diabetic cardiomyopathy. *Diabetes*. 61(3):716–727. <https://doi.org/10.2337/db11-0477>
- Renard J, Krebs MO, Jay TM, Le Pen G (2013) Long-term cognitive impairments induced by chronic cannabinoid exposure during adolescence in rats: a strain comparison. *Psychopharmacology* 225(4):781–790. <https://doi.org/10.1007/s00213-012-2865-z>
- Rosado T, Gonçalves J, Luís Â, Malaca S, Soares S, Vieira DN, et., al. (2018) Synthetic cannabinoids in biological specimens: a review of current analytical methods and sample preparation techniques. *Bioanalysis* 10(19):1609–1623. <https://doi.org/10.4155/bio-2018-0150>
- Sánchez MG, Ruiz-Llorente L, Sánchez AM, Díaz-Laviada I (2003) Activation of phosphoinositide 3-kinase/PKB pathway by CB(1) and CB(2) cannabinoid receptors expressed in prostate PC-3 cells. Involvement in Raf-1 stimulation and NGF induction. *Cell Signal* 15(9):851–859. [https://doi.org/10.1016/s0898-6568\(03\)00036-6](https://doi.org/10.1016/s0898-6568(03)00036-6)
- Sim-Selley LJ, Schechter NS, Rorrer WK, Dalton GD, Hernandez J, Martin BR, Selley DE (2006) Prolonged recovery rate of CB1 receptor adaptation after cessation of long-term cannabinoid administration. *Mol Pharmacol* 70(3):986–996. <https://doi.org/10.1124/mol.105.019612>
- Singh S, Filion KB, Abenhaim HA, Eisenberg MJ (2020) Prevalence and outcomes of prenatal recreational cannabis use in high-income countries: a scoping review. *BJOG*. 127(1):8–16. <https://doi.org/10.1111/1471-0528.15946>
- Slavic S, Lauer D, Sommerfeld M, Kemnitz UR, Grzesiak A, Trappiel M et al (2013) Cannabinoid receptor 1 inhibition improves cardiac function and remodeling after myocardial infarction and in experimental metabolic syndrome. *J Mol Med (Berl)* 91(7):811–823. <https://doi.org/10.1007/s00109-013-1034-0>
- Tomiyama K, Funada M (2011) Cytotoxicity of synthetic cannabinoids found in "spice" products: the role of cannabinoid receptors and the caspase cascade in the NG 108-15 cell line. *Toxicol Lett* 207(1):12–17. <https://doi.org/10.1016/j.toxlet.2011.08.021>
- Tomiyama K, Funada M (2014) Cytotoxicity of synthetic cannabinoids on primary neuronal cells of the forebrain: the involvement of cannabinoid CB1 receptors and apoptotic cell death. *Toxicol Appl Pharmacol* 274(1):17–23. <https://doi.org/10.1016/j.taap.2013.10.028>
- Wang S, Zhu Q, Liang G, Franks T, Boucher M, Bence KK et al (2021) Cannabinoid receptor 1 signaling in hepatocytes and stellate cells does not contribute to NAFLD. *J Clin Invest* 131(22):e152242. <https://doi.org/10.1172/JCI152242>
- Weinstein AM, Rosca P, Fattore L, London ED (2017) Synthetic cathinone and cannabinoid designer drugs pose a major risk for public health. *Front Psychiatry* 8:156. <https://doi.org/10.3389/fpsy.2017.00156>
- Yassa HA, Dawood Ael W, Shehata MM, Abdel-Hady RH, Aal KM (2010) Subchronic toxicity of cannabis leaves on male albino rats. *Hum Exp Toxicol* 29(1):37–47. <https://doi.org/10.1177/0960327109354312>

Publisher's Note

Springer Nature remains neutral with regard to jurisdictional claims in published maps and institutional affiliations.